Robophysical modeling of bilaterally activated and soft limbless locomotors[*]

Perrin E. Schiebel[1], Marine C. Maisonneuve[1], Kelimar Diaz, Jennifer M. Rieser, and Daniel I. Goldman

Georgia Institute of Technology, Atlanta GA 30332 USA
daniel.goldman@physics.gatech.edu

Abstract. Animals like snakes use traveling waves of body bends to move in multi-component terrestrial terrain. Previously we studied [Schiebel et al., *PNAS*, 2019] a desert specialist, *Chionactis occipitalis*, traversing sparse rigid obstacles and discovered that passive body buckling, facilitated by unilateral muscle activation, allowed obstacle negotiation without additional control input. Most snake robots have one motor per joint whose positions are precisely controlled. In contrast, we introduce a robophysical model designed to capture muscle morphology and activation patterns in snakes; pairs of muscles, one on each side of the spine, create body bends by unilaterally contracting. The robot snake has 8 joints and 16 motors. The joint angle is set by activating the motor on one side, spooling a cable around a pulley to pull the joint that direction. Inspired by snake muscle activation patterns [Jayne, J. *Morph.*, 1988], we programmed the motors to be unilaterally active and propagate a sine wave down the body. When a motor is inactive, it is unspooled so that its wire cannot generate tension. Pairs of motors can thus resist forces which attempt to lengthen active wires but not those pushing them shorter, resulting in a kinematically soft robot that can be passively deformed by the surroundings. The robot can move on hard ground when drag anisotropy is large, achieved via wheels attached to the bottom of each segment, passively re-orient to track a wall upon a head-on collision, and traverse a multi-post array with open loop control facilitated by buckling and emergent reversal behaviors. In summary, we present a new approach to design limbless robots, offloading the control into the mechanics of the robot, a successful strategy in legged robots [Saranli et al., *IJRR*, 2001].

Keywords: Snake Robot · Complex Terrain · Passive Dynamics

1   Introduction

The elongate, limbless body plan seen in organisms like snakes is versatile, facilitating locomotion in habitats ranging from aquatic to arboreal [5]. This adaptability makes limbless locomotion an attractive strategy for robots, especially those intended for tasks like search and rescue where the surroundings can be confined or unstable. However, this mode of locomotion requires coordinating a high degree-of-freedom body, a task which is further complicated by the addition of environmental heterogeneities.

There are two broad classes for the treatment of terrain heterogeneities in snake robots; obstacle avoidance [6] and obstacle-aided locomotion [29]. A challenge to both classes is obstacles that cause forces resisting forward motion. Traditional snake robots have one motor per joint ([21, 7, 16], Fig. 1A), and thus must use sensing and control strategies to avoid deleterious terrain interactions.

Ensuring useful robot coordination while bypassing obstacles generally requires sophisticated control. For example, Transeth et al. [29] developed a hybrid model to determine joint trajectories for obstacle aided locomotion. Computation can be simplified in some cases by using a lower-dimensional intermediary between motion planning and control such as shape functions [30] or virtual functional segments [22]. Decentralized control, inspired by biological central pattern generators [9], can further reduce central control complexity by offloading computation to local reflexes, whether to avoid obstacles [31], adapt to changes in the environment [10, 25], or use obstacles for propulsion [13, 14]. These strategies make use of knowledge of the terrain in a closed-loop control. Robots can collect this information using vision [18], contact sensing [31, 28, 2], contact force sensing [15], or joint-torque measurements [30].

In contrast to most limbless robots, snakes articulate their joints using bilateral musculature. The lateral body bends the animals use to generate propulsion during terrestrial locomotion are achieved by alternating unilateral activation of the epaxial muscles (Fig. 1B) [12].

We previously studied the desert-dwelling Shovel-nosed snake, *Chionactis occipitalis* (Fig. 1C), which uses a stereotyped serpenoid waveform (sinusoidally varying curvature) to move quickly (but non-inertially [26]) across its natural habitat consisting of a sandy substrate and sparse heterogeneities like rocks, twigs, and plants [17, 26]. We found evidence that this snake used a control strategy in which it targeted the muscle activation pattern for a waveform that allowed fast motion on the granular substrate and did not change this pattern in response to collisions with the surroundings. Our study suggested that this "open-loop" movement was facilitated by unilaterally activated muscles which allowed the body to be passively deformed by the surroundings (Fig. 1D, [27]). This work indicated that a similar unilateral activation scheme could aid snake-like robots in navigating obstacles without the need for sensing or control which responds to the surroundings.

Addition of mechanical compliance can help prevent robots from becoming jammed in obstacles. This has typically been achieved by adding a torsional spring element to the actuators [25, 21, 23]. As these robots are still driven by a
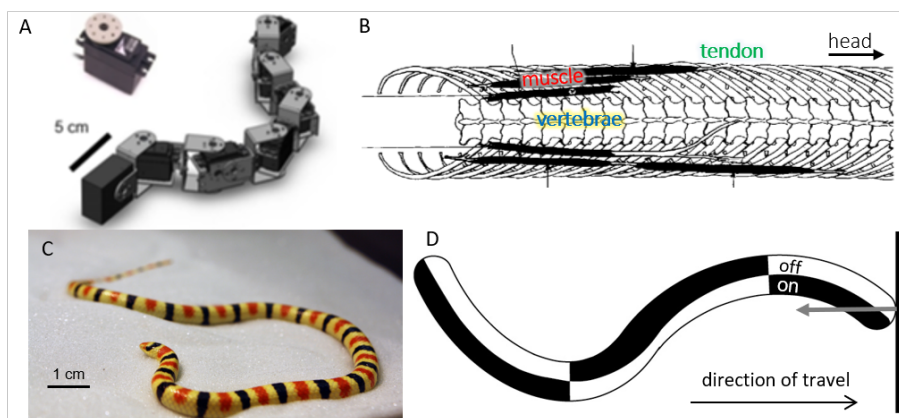
Fig. 1. Types of actuation in limbless locomotors. (A) CAD model of a limbless robot made of rigidly linked servomotors. Inset is a single motor used to bend the joints both left and right. (B) Simplified snake anatomy that illustrates musculoskeletal system used to create lateral body bends. From [5] (C) *C. occipitalis* on a model desert sand (297±40 μm glass particles) in the laboratory. (D) Cartoon of muscle activation and asymmetric compliance. Black areas are active muscles, white are inactive. Muscle segments transition from "on" to "off" at the apexes of the waveform. When the animal experiences external forces, e.g. the gray arrow, the body buckles toward active muscles.

single actuator per joint, however, directional compliance such as observed in the animal can only be achieved using active feedback. Further, when deformed away from its resting shape the compliant spring element will exert torque resisting the external force.

Our goal was to develop a robophysical model that captured the bilateral compliance of the snake. The design target was a robot that would be able to successfully execute snake-like waveforms and would offer very little resistance to forces acting to bend the joints toward active motor units. We began by simplifying to a pair of actuators per joint, one on either side, spanning a single joint (Fig. 2). Each individual actuator, like a muscle, can only act to close the joint in one direction. By working in tandem the actuator pairs bend the joint both directions.

We used our robophysical model to test the bilateral actuation scheme. The device was able to mimic the waveform of the biological snake to translate across a homogeneous substrate by using wheels to provide the necessary anisotropic forces [8, 20]. The bilaterally-actuated robot passively re-orients its direction of motion when encountering a solid wall. Further, the robot is able to navigate a hexagonal lattice without feedback from the environment, by passively buckling and reversing. This indicates the utility of such a scheme in aiding limbless locomotion in complex terrains.

2   Materials and Methods

The robot consists of nine 3D printed segments attached by eight pin joints and 16 actuators, one on each side of every joint (Fig. 2A). The robot was modular such that segments could be added, subtracted, or replaced as needed. The bottom of each joint was designed to interface with LEGO blocks so that the robot-ground contact could be easily changed. For this experiment, we used LEGO wheels to create the anisotropic force needed for effective undulatory locomotion [8].

Each segment had a rigid midline and two curved side lobes that supported the motors, provided an attachment point for the Kevlar thread cables, and served to protect the cables from the surroundings. On the top of each side lobe there was a motor adapter. A joint consisted of two segments and two motor/pulley/thread assemblies, one on each side (Fig. 2). The joints could freely rotate in the horizontal plane but were designed to limit off-axis motion. Thus the robot's shape changes were largely constrained to two dimensions, although some vertical bending was observed, as further discussed below. Each segment had a holder for an IR reflective marker, and an OptiTrack motion capture system (Natural Point) tracked the position of the markers.

Inoue et al. [11] developed a biologically-inspired robot with bilateral actuation using McKibben-type actuators. The goal of the McKibben-actuated robot was to model the muscle morphology and dynamics of the animal as closely as possible. Our interest was to understand how the passive mechanical properties of the bilateral activation scheme facilitates navigating obstacles. For this purpose our robot has the advantage of an easily reconfigurable 3D printed design and the thread offers negligible resistance to compressive forces.

The target waveform for the robot's joint angles, ζ_i (Fig. 2C), was a *serpenoid curve* [6], $\zeta_i(t) = \zeta_{max} sin(ks_i + 2\pi f t)$. $k = 1$ is the spatial frequency, $f = 0.3$ Hz is the undulation frequency, and $\zeta_{max} = 0.87$ radians is the maximum joint angle. We chose to have one wave on the body, as this was few enough waves to be resolved with the number of joints but was also sufficient for forward motion without excessive slipping or over-torquing motors.

The motor-pulley-thread actuators had two states, actively shortening and passively lengthening, in which the motors were spooling and unspooling thread, respectively. On the active side the motor tracked the serpenoid joint angle positions, spooling the thread to reduce the gap between the pulley and adjacent segment's side lobe (Fig. 2C, red "on" cable). The change between active and passive occurred when the thread was maximally shortened, at peaks of the sinusoidal wave[1]. When a motor changed from active to passive, it would rapidly unspool to a set position where the joint could fully close without causing tension on the thread (Fig. 1C, black "off" cable). While the current study was focused on unilateral activation, this setup allowed for bilateral actuation as well and thus could be also used to explore co-contraction.

---

[1] The sign of the commanded joint angle velocity was used to determine state.
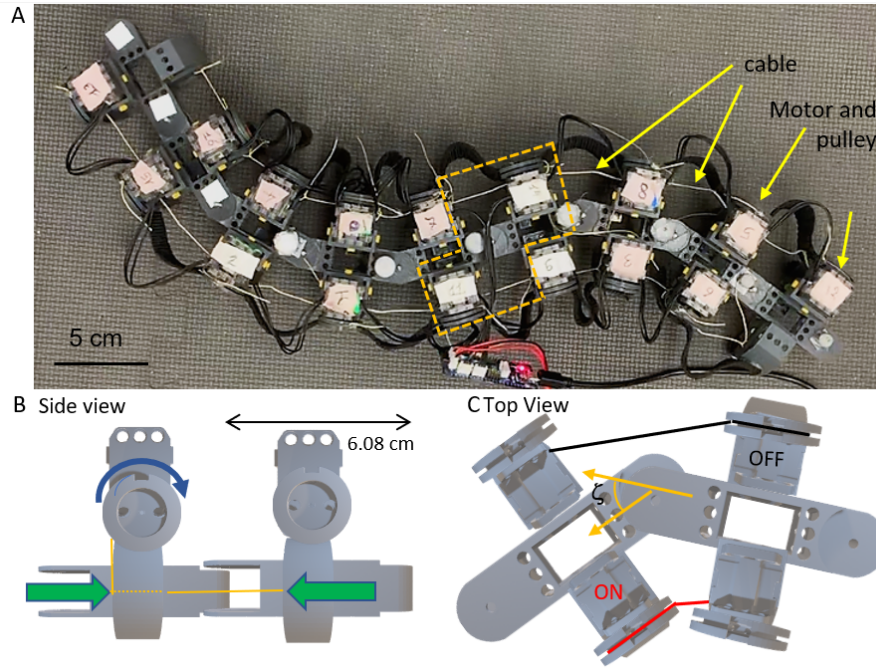
Fig. 2. Two-actuator-joint design for a biarticulated limbless robot. (A) Top down view of the robot on a rubber mat. Yellow dashed line encloses one joint unit. Note that the hemispherical head is seen in Fig. 4A. (B) Side view of the CAD model of a joint made of two segments. Cable path illustrated in yellow. The cable is affixed to the side lobe of one segment, passes through a hole in the lobe of the neighboring segment, and winds around the pulley. When the motor spools the cable in the direction indicated by the blue arrow, the cable generates force as shown by the green arrows. (C) Top view. The red and black lines are a cartoon of the cable on the actively spooling motor and inactive unspooled motor, respectively. Yellow arrows indicate the angle ζ between adjacent segments.

We measured the relationship between commanded motor position and resulting joint angle (Fig. 3A). The relationship was predominantly linear, although there was some systematic deviation. For the current work we chose to use the linear relationship to control the robot.

It was necessary to empirically adjust the cable lengths so that each joint had the same range of motion. This was done by hand, such that there was some discrepancy between how well different joints tracked the commanded signal (Fig. 3B). Nevertheless, the current robot successfully tracked the commanded angles (Fig. 3D), leading to snake-like locomotion across a rubber mat substrate (Fig. 3C-F, forces generated by the wheels on this substrate are similar to those acting on a snake trunk segment moving through sand [20]). Importantly, like the sand-swimming snake studied in [26, 27], the robot's dynamics were highly over-
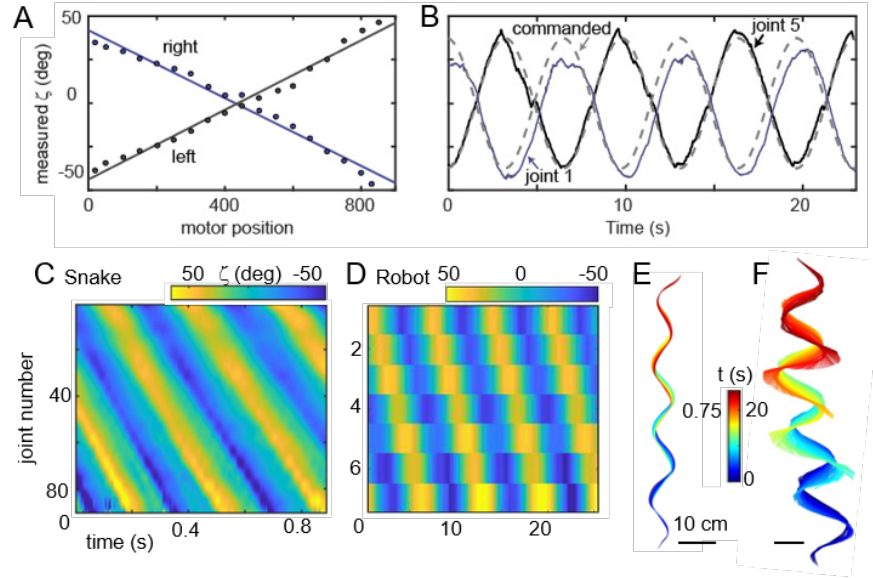
Fig. 3. Robot moves using lateral undulation (A) Robot joint ζ as a function of the commanded motor positions. Two motors are shown, one which bends its joint left (blue markers and line), and one which bends right (black markers and line). Lines are linear fits to the data. Slopes ± 0.1 and intercepts $+42.0$ and -43.9 for left and right motor, respectively ($R^2 = 0.98$ for both). (B) ζ as a function of time. Shown are joints 1 (light purple curve) and 5 (black curve). The commanded trajectory for each joint is a gray, dashed line. (C) Spacetime plot of ζ measured on the snake. We used a cubic-spline interpolant to upsample tracked points as in [26]. Note joint numbers are less than the number of snake vertebrae. (D) Spacetime plot of ζ measured on the robot. (E) Tracked snake midlines as the animal moves across the model desert sand, colored by time. (F) Tracked robot midlines on mat with wheels, colored by time.

damped; if it stopped self-deforming, it rapidly stopped translating (see analysis of a similar propulsion scheme in [19]).

We next added a hemispherical head to the first joint so that the robot would not contact obstacles with a flat surface (see Fig. 4B). However, adding the head was unexpectedly detrimental to the robot's ability to remain coordinated and perform the serpenoid curve. Surprisingly, adding a 200 g weight between the head and the first joint resulted in coordination and effective locomotion. Observing the robot from the side, we noticed that when the robot was moving either without the head or with the head plus the additional mass, the segments at the curve apexes would slightly lift off the ground. This *sinus lifting* is observed in biological snakes [8, 26] and serves to remove those segments which are not generating thrust from contact with the substrate. The robot with only the head and no added mass did not exhibit the lifting kinematics. Our hypothesis

was that the mass of the head generated torque that prevented the motors from lifting segments, and torque from the added mass countered that of the head.

3   Results and Discussion

We sought to discover if the open-loop robot could body-buckle like the animal (e.g. Fig. 4A, t=117 ms) during head-on collision with a wall, and whether it would re-orient to travel along the wall without using feedback. Wall following has been studied from a neuromechanical perspective in invertebrate (cockroach) locomotion [4], with feedback control playing a critical role in task performance.

We used a vertically oriented whiteboard as a wall (Fig. 4B). The low-friction surface of the whiteboard simplified the system so that the robot was primarily experiencing ground contact forces and wall normal forces. The substrate was a smooth wooden surface. While we initially explored robot locomotion on a rubber mat (Fig. 2A) that facilitated low-slip motion, we found impurities in the substrate (ridges for grip) could cause the waveform to deform. While slipping of the robot was higher on the wooden surface it allowed us to more easily observe wall-induced changes to the waveform.

The robot was initially placed with its long axis perpendicular to the wall (Fig. 4B, t=-2 s). The robot's position was randomly chosen between each trial to vary the phase of the wave and position of the head when it contacted the wall. In all cases the robot performed at least one full cycle of the waveform before contacting the wall. The experiment would stop when the long axis of the robot was fully parallel to the wall. The snake data was from [27]. In these experiments the animal moved freely across the model granular substrate into a vertical whiteboard wall.

The robot began by moving across the substrate using the serpenoid waveform (Fig. 4B, t=-2 s) similar to that used by the snake (Fig. 4A, t=-64 ms). The robot initially deformed under external forces from the wall, with large amplitude curves appearing on the body (Fig. 4B, t=4.5 s). The animal also deformed, leading to areas of high curvature (Fig. 4A, t=117 ms).

Unlike the snake, in some robot trials we initially observed a straightening behavior after impact (Fig. 4B, t=0 s) and the increased amplitude became apparent after half a cycle (Fig. 4B, t=1-4.5 s). After this initial interaction the front of the robot began to turn until the anterior segments were parallel to the wall (Fig. 4B, t=8 s). If at this point the robot was not re-oriented sufficiently to continue along the wall, the same process would repeat one or more times (note head turning back into the wall at Fig. 4B, t=10 s). Once the robot was rotated enough, it returned to its initial waveform and amplitude (Fig. 4B, t=13 s).

While both the snake and robot turned to travel along the wall (Fig. 4C), this process required more gait cycles in the robot. We characterized the number of undulations the robot underwent before it successfully turned (defined as 70% of the body parallel to the wall). The robot took on average 2.4±0.6 undulation cycles to reorient (Fig. 4D). The animal never required more than one undulation, instead the body would buckle until the anterior end of the trunk was parallel
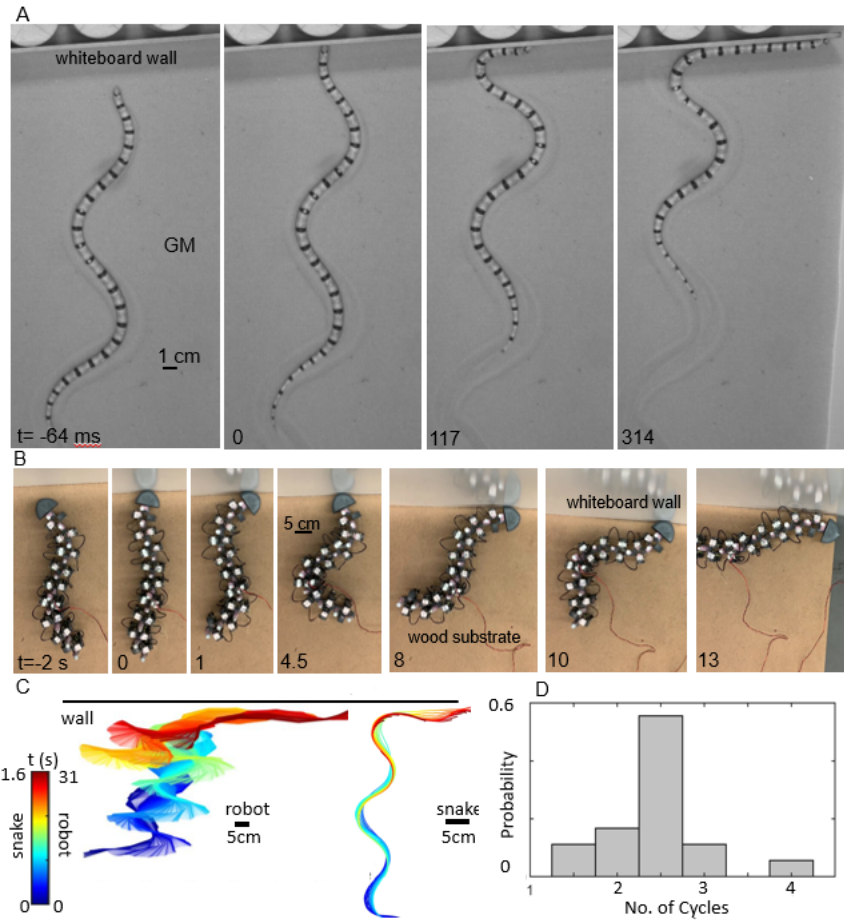
Fig. 4. Passive undulatory re-orientation during wall collisions. (A) The shovel-nosed snake *C. occipitalis* snake travels up the page on the model desert sand. The nose of the snake contacts the wall at t=0 ms. Time relative to contact is shown above each frame. (B) Snake robot travels up the page on the wood substrate. Time is labelled above each from relative to the initial wall contact occurring at t=0 s. (C) Tracked midlines of example robot (*left*) and snake (*right*) trials, colored by time. Wall location indicated by black line. (D) Probability for the number of cycles needed for the robot to execute a 90 degree turn after the wall collision (defined as 70 percent of the robot's long axis parallel to the wall). 18 trials included.

to the wall (Fig. 4B, t = 314 ms) after which the snake would change behavior. The animals either explored the wall with the nose or vaulted the front of the body off the substrate to climb over it. The robot demonstrates that changing behavior is not necessary to passively reorient after collision. However, it may be that changing strategy after the initial buckling is desirable. For example, to reverse the direction change caused by the obstacle.

While both the robot and snake body buckled after collision with the wall (Fig. 4A, t=4.5 s and Fig. 4B, t=117 ms), the snake would bend to higher curvatures. The animal has more joints and a higher aspect ratio (length divided by width) than the robot. Increasing the number of joints increases the available resolution while increasing aspect ratio allows higher curvature bends before self-intersection of the body. The snakes' morphology thus allowed it to use more waves along the body (average wavenumber on the surface of granular matter is 1.9 waves [26]). We hypothesize that this allows the posterior portions of the body to continue providing thrust while the front portion is being buckled by the environmental forces.

We note that, even in our setup where the robot-terrain friction was low-enough that the robot's wheels would slip relative to the substrate, we still observed buckling of the joints. This was because our mechanical design offered very little resistance, less than the other forces acting on the robot, to buckling toward active motors.
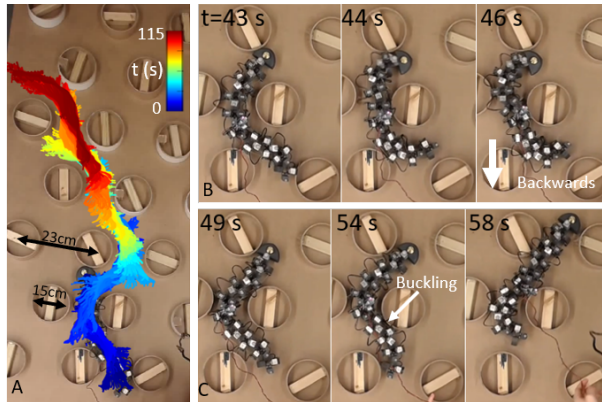
Fig. 5. Passive buckling and reversals facilitate open-loop traversal of a model cluttered terrain. (A) Tracked robot midlines as the robot moves up the page, colored by time. (B) Robot passive backing behavior in the lattice. Time is labelled above each frame. (C) Robot passive buckling behavior in the lattice. Time is labelled above each frame.

We next tested our robot in a simplified model for heterogeneous terrain, a regular array of posts rigidly affixed to a wood substrate (Fig. 5A). The robot was able to traverse the lattice with open-loop control, without any knowledge of its surroundings (Fig. 5A). The post diameter, 15cm, was chosen to be large enough so that posts could not fit between the robot's joints and interfere with the thread. When the robot entered configurations where forces from the posts

prevented forward motion (e.g. Fig. 5B,C), the passive mechanism helped resolve jams.

Buckling behavior, previously seen in the wall collision assay (Fig. 5C), was observed when the robot was jammed between posts. At t = 49 s in Fig. 5C the robot is jammed between four posts and the robot is unable to progress. At 54 s the force from the rightmost post buckles the body, allowing the robot to reposition itself and resume the nominal waveform, continuing past the top post by t = 58 s.

An emergent reversal behavior occurred when jamming deformed the waveform in a way that it did not provide sufficient propulsion. In Fig. 5C at t = 43-44 s the robot is stuck between several posts in a configuration that disallows the nominal waveform. At 46 s the front of the robot has moved slightly backward, allowing the head to progress around the post as seen at 49 s.

Unlike the control schemes used to prevent jamming in traditional snake robots [30], our robot was able to solve jams without sensing the obstacles or changing the motor activation pattern. However, this strategy did typically require multiple undulation cycles to become unstuck, and was not always successful. A trial was ended if for 10 undulations the robot was unable to progress. In 2/6 trials the robot did not progress.

Future work can characterize the genesis of the unsolvable jams. This can inform whether changes to the robot, such as increasing the number of joints and the maximum joint angles to give the robot greater flexibility more akin to that of the biological snake, will extend the situations where the purely passive mechanism can contend with adverse heterogeneities. Further study can also determine whether the robot without wheels can use the posts for propulsion as well as in which situations a more sophisticated sensing and control program is needed.

4   Conclusion

Here, we present a novel snake robot that relies on a two-actuator joint scheme to model bilateral muscle activation patterns seen in snakes [12]. Our robot is completely open loop, passively deforming and adapting to the environment without sensing or control. By offloading the control into the mechanics of the robot, a successful strategy in legged robots [24], our robot can capture snake-like behavior (e.g. buckling) and navigate complex terrain.

The two-actuator-joint scheme was able to mimic snake locomotion when freely moving while also allowing snake-like passive body buckling. We note the wall following scheme that emerges in our snake robot requires no feedback; in this way it complements the work of [4]. We posit that the wall following could be aided via addition of head contact sensing with a amplitude modulated turning scheme [1]. Further, our robot was able to traverse a multi-post array, resolving jams with passive body buckling and emergent backing behaviors.

While our work has drawn inspiration from snakes, many animals across different environments and length scales rely on undulatory locomotion, using

bilateral activation of their muscles to generate and propagate waves along their body (e.g. *C. elegans* [3]). Therefore, we can use our robot (whose dynamics are highly damped [20]) to test the bilateral actuation scheme in undulators across different length scales and terrains. We expect that future limbless robots can take advantage of the principles discovered in our robophysical model.

References

1. Astley, H.C., Rieser, J.M., Kaba, A., Paez, V.M., Tomkinson, I., Mendelson, J.R., Goldman, D.I.: Side-impact collision: Mechanics of obstacle negotiation in sidewinding snakes. bioRxiv (2020)
2. Bayraktaroglu, Z.Y., Kilicarslan, A., Kuzucu, A., Hugel, V., Blazevic, P.: Design and control of biologically inspired wheel-less snake-like robot. In: The First IEEE/RAS-EMBS International Conference on Biomedical Robotics and Biomechatronics, 2006. BioRob 2006. pp. 1001–1006. IEEE (2006)
3. Butler, V.J., Branicky, R., Yemini, E., Liewald, J.F., Gottschalk, A., Kerr, R.A., Chklovskii, D.B., Schafer, W.R.: A consistent muscle activation strategy underlies crawling and swimming in caenorhabditis elegans. Journal Royal Society Interface **12**(102) (2014)
4. Cowan, N.J., Lee, J., Full, R.J.: Task-level control of rapid wall following in the american cockroach. J. Exp. Bio. **209**(9), 1617–1629 (2006)
5. Gans, C.: Locomotion of limbless vertebrates: pattern and evolution. Herpetologica **42**(1), 33–46 (1986)
6. Hirose, S.: Biologically Inspired Robots: Snake-Like Locomotors and Manipulators. Oxford University Press (1993)
7. Hopkins, J.K., Spranklin, B.W., Gupta, S.K.: A survey of snake-inspired robot designs. Bioinspiration & biomimetics **4**(2), 021001 (2009)
8. Hu, D.L., Nirody, J., Scott, T., Shelley, M.J.: The mechanics of slithering locomotion. Proc. Nat. Acad. Sci. USA **106**(25), 10081–10085 (2009)
9. Ijspeert, A.J.: Central pattern generators for locomotion control in animals and robots: a review. Neural networks **21**(4), 642–653 (2008)
10. Ijspeert, A.J., Crespi, A., Ryczko, D., Cabelguen, J.M.: From swimming to walking with a salamander robot driven by a spinal cord model. science **315**(5817), 1416–1420 (2007)
11. Inoue, K., Nakamura, K., Suzuki, M., Mori, Y., Fukuoka, Y., Shiroma, N.: Biological system models reproducing snakes' musculoskeletal system. In: 2010 IEEE/RSJ International Conference on Intelligent Robots and Systems. pp. 2383–2388. IEEE (2010)
12. Jayne, B.C.: Muscular mechanisms of snake locomotion: an electromyographic study of lateral undulation of the florida banded water snake (nerodia fasciata) and the yellow rat snake (elaphe obsoleta). Journal of Morphology **197**(2), 159–181 (1988)
13. Kano, T., Ishiguro, A.: Obstacles are beneficial to me! scaffold-based locomotion of a snake-like robot using decentralized control. In: 2013 IEEE/RSJ International Conference on Intelligent Robots and Systems. pp. 3273–3278. IEEE (2013)
14. Kano, T., Yoshizawa, R., Ishiguro, A.: Tegotae-based decentralised control scheme for autonomous gait transition of snake-like robots. Bioinspiration & biomimetics **12**(4), 046009 (2017)

15. Liljeback, P., Pettersen, K.Y., Stavdahl, Ø., Gravdahl, J.T.: Experimental investigation of obstacle-aided locomotion with a snake robot. IEEE Transactions on Robotics **27**(4), 792–800 (2011)
16. Liljebäck, P., Pettersen, K.Y., Stavdahl, Ø., Gravdahl, J.T.: A review on modelling, implementation, and control of snake robots. Robotics and Autonomous Systems **60**(1), 29–40 (2012)
17. Mosauer, W.: Locomotion and diurnal range of sonora occipitalis, crotalus cerastes, and crotalus atrox as seen from their tracks. Copeia **1933**(1), 14–16 (1933)
18. Ponte, H., Queenan, M., Gong, C., Mertz, C., Travers, M., Enner, F., Hebert, M., Choset, H.: Visual sensing for developing autonomous behavior in snake robots. In: 2014 IEEE International Conference on Robotics and Automation (ICRA). pp. 2779–2784. IEEE (2014)
19. Rieser, J.M., Schiebel, P.E., Pazouki, A., Qian, F., Goddard, Z., Wiesenfeld, K., Zangwill, A., Negrut, D., Goldman, D.I.: Dynamics of scattering in undulatory active collisions. Physical Review E **99**(2), 022606 (2019)
20. Rieser, J.M., Schiebel, P.E., Pazouki, A., Qian, F., Goddard, Z., Zangwill, A., Negrut, D., Goldman, D.I.: Collision-induced scattering of a self-propelled slithering robot. arXiv preprint arXiv:1712.00136 (2017)
21. Rollinson, D., Bilgen, Y., Brown, B., Enner, F., Ford, S., Layton, C., Rembisz, J., Schwerin, M., Willig, A., Velagapudi, P., et al.: Design and architecture of a series elastic snake robot. In: 2014 IEEE/RSJ International Conference on Intelligent Robots and Systems. pp. 4630–4636. IEEE (2014)
22. Sanfilippo, F., Azpiazu, J., Marafioti, G., Transeth, A.A., Stavdahl, Ø., Liljebäck, P.: Perception-driven obstacle-aided locomotion for snake robots: the state of the art, challenges and possibilities. Applied Sciences **7**(4), 336 (2017)
23. Sanfilippo, F., Helgerud, E., Stadheim, P.A., Aronsen, S.L.: Serpens: A highly compliant low-cost ros-based snake robot with series elastic actuators, stereoscopic vision and a screw-less assembly mechanism. Applied Sciences **9**(3), 396 (2019)
24. Saranli, U., Buehler, M., Koditschek, D.E.: Rhex: A simple and highly mobile hexapod robot. The International Journal of Robotics Research **20**(7), 616–631 (2001)
25. Sato, T., Kano, T., Ishiguro, A.: On the applicability of the decentralized control mechanism extracted from the true slime mold: a robotic case study with a serpentine robot. Bioinspiration & biomimetics **6**(2), 026006 (2011)
26. Schiebel, P.E., Astley, H.C., Rieser, J.M., Agarwal, S., Hubicki, C., Hubbard, A.M., Cruz, K., Mendelson, J., Kamrin, K., Goldman, D.I.: Mitigating memory effects during undulatory locomotion on hysteretic materials. bioRxiv p. 748186 (2019)
27. Schiebel, P.E., Rieser, J.M., Hubbard, A.M., Chen, L., Rocklin, D.Z., Goldman, D.I.: Mechanical diffraction reveals the role of passive dynamics in a slithering snake. Proc. Nat. Acad. Sci. USA **116**(11), 4798–4803 (2019)
28. Tanaka, M., Kon, K., Tanaka, K.: Range-sensor-based semiautonomous whole-body collision avoidance of a snake robot. IEEE Transactions on Control Systems Technology **23**(5), 1927–1934 (2015)
29. Transeth, A.A.: Snake Robot Obstacle-Aided Locomotion: Modeling, Simulations, and Experiments. IEEE Transactions on Robotics **24**(1), 88–104 (Feb 2008)
30. Travers, M.J., Whitman, J., Schiebel, P., Goldman, D., Choset, H.: Shape-based compliance in locomotion. In: Robotics: Science and Systems (2016)
31. Wu, X., Ma, S.: Neurally controlled steering for collision-free behavior of a snake robot. IEEE Transactions on Control Systems Technology **21**(6), 2443–2449 (2013)